Temperature Shifting of Convergent Flow Measured Effective Elongational Viscosity

John R. Collier, Simioan Petrovan, Parag Patil

Chemical Engineering Department, University of Tennessee, Knoxville, Tennessee 37996-2200

Received 26 February 2002; accepted 16 April 2002

ABSTRACT: The effective elongational viscosity data on a series of polyolefins as a function of temperature are shifted to a reference temperature using the approach for shifting shearing viscosity data. The temperature shift factors are obtained from complex and capillary shear rheology, and these are the same factors used for shifting the shear rheology. A Carreau rheological model was used to determine the zero shear rate viscosity at different temperatures, and an Arrhenius expression was used to determine the temperature shift factors. The same shift factors are shown to produce separate master curves for shear and elongational rheology at reference temperatures. The commercial grades of polyolefins studied include an extrusion grade of polypropylene and metallocene and conventionally catalyzed low and high density polyethylene materials. © 2002 Wiley Periodicals, Inc. J Appl Polym Sci 87: 1387–1396, 2003

Key words: elongational viscosity; semihyperbolic die; shift factor; master curve; temperature shifting; activation energy for flow; low density polyethylene; high density polyethylene; polypropylene

INTRODUCTION

The effective elongational viscosity of polymer melts and concentrated solutions can be determined using flow through convergent dies as demonstrated elsewhere.[1–4] The semihyperbolic dies (Fig. 1) are special dies[5,6] for which the radius (r) of the flowing channel is given by eq. (1):

$$r^2 = \frac{C}{z + B} \tag{1}$$

where C and B are two constants, depending on the inlet and outlet diameters of the die channel. The flow rate (Q) can be calculated with eq. (2):

$$Q = \pi r^2 \nu_z \tag{2}$$

In eqs. (3) and (4) the velocities are given in which Ψ and Φ are the stream function and potential function, respectively, for this type of flow as given elsewhere:[1]

$$\nu_z = -\frac{1}{r}\left(\frac{\partial \Psi}{\partial r}\right) = -\frac{\partial \Phi}{\partial z} = \dot{\varepsilon} z \tag{3}$$

$$\nu_r = \frac{1}{r}\left(\frac{\partial \Psi}{\partial z}\right) = -\frac{\partial \Phi}{\partial r} = -\frac{\dot{\varepsilon}}{2} r \tag{4}$$

Correspondence to: J. R. Collier (collier@utk.edu).

Journal of Applied Polymer Science, Vol. 87, 1387–1396 (2003)

The elongational strain rate ($\dot{\varepsilon}$) can be calculated and is given by eq. (5):

$$\dot{\varepsilon} = \frac{d\nu_z}{dz} = \frac{Q}{\pi C} \tag{5}$$

Therefore, the main feature of the semihyperbolic die is that the elongational strain rate along the channel is constant. Using this fact and doing a momentum, mass, and energy balance, the theoretical development for the calculation of the effective elongational viscosity (η_{eff}) leads to eq. (6):

$$\eta_{\text{eff}} = -\frac{\Delta P}{\dot{\varepsilon}\varepsilon_{\text{H}}} \tag{6}$$

where ΔP is the pressure drop along the die and ε_{H} is the Hencky strain, which is defined by the equation

$$\varepsilon_{\text{H}} = \ln\left(\frac{D_0}{D_e}\right)^2 \tag{7}$$

and represents the flow cross-sectional area reduction due to the semihyperbolic shape of the channel. Details on the experimental technique for the measurement of the elongational viscosity by using hyperbolic convergent dies are given elsewhere.[1]

The viscosity values obtained using a semihyperbolic convergent die are apparent elongational viscosities rather than true elongational viscosities because they are dominated by the influence of the body forces

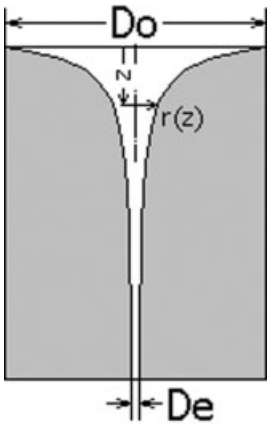

Figure 1 The geometry of the semihyperbolic die channel.

in the polymer melt and solution that must be overcome to develop orientation during this convergent flow. These effective elongational viscosities are therefore related to the orientability or resistance to orientation development of polymer melts and solutions. As we showed previously,[1] the body forces opposing orientation are 3 orders of magnitude higher in an extrusion grade of polypropylene (PP) than the shearing forces at the wall. Furthermore, the effective elongation viscosity for this PP was the same whether or not the PP was encased in a sheath of low viscosity polyethylene (PE). When orientable polymer melts and solutions are formed in free boundary regions by the application of tensile forces, the shape of the attenuating fiber will approach that of the semihyperbolic die shape as substantiated by the nearly constant elongational strain rate experienced under isothermal conditions. Because higher degrees of orientation can be imposed when the polymer melt or solution is forced to contract into the semihyperbolic shape (by either the geometry or mass balance in free surface flow), the body forces must be overcome; therefore, the effective elongational viscosity is a maximum with regard to shape. If a convergent flow is allowed to occur because of a geometric consideration that is less severe than semihyperbolic (e.g., a linear convergent geometry), then vorticity and internal recirculation can more readily occur and not force the molecules to develop as much orientation. Similar effects occur in orientation development in planar geometries. Flow in the semihyperbolic convergent dies is in a Eulerian steady state that can be considered to be a quasistable thermodynamic state.

BACKGROUND

Temperature related shifting of shear rheology

The shifting of the shear viscosity versus the shear strain rate, which is taken at different temperatures to a master curve at a reference temperature, can be done by using the so-called method of reduced variables.[7] It is accomplished by determining a shift factor (a_T). The literature presents an abundance of master curves for shear viscosity and some other properties like dynamic moduli or first normal stress difference. In the following we present the fundamentals of shear viscosity shifting to show that it can also be applied for shifting the elongational viscosity, because the literature on this topic is rather scarce.

If a zero shear rate viscosity can be obtained, then the viscosity in the Newtonian region is not a function of the shear strain rate ($\dot{\gamma}$) in the low shear strain rate region, and a_T can be measured directly by the ratio of viscosities in this region with respect to temperature. The value of a_T is given by eq. (8):[8,9]

$$a_T = \frac{\lambda_j(T)}{\lambda_j(T_0)} = \frac{\eta_0(T)T_0\rho_0}{\eta_0(T_0)T\rho} \tag{8}$$

where T is the measurement temperature, T_0 is the reference temperature to which the data is being shifted, $\lambda_j(T)$ is the relaxation time of the jth Rouse chain at T, and $\lambda_j(T_0)$ is the relaxation time of the jth Rouse chain at T_0. Because all of the chains have a similar response, it is used for polymer melts and solutions. For polymer solutions the η_0 terms are replaced by $\eta_0 - \eta_s$, where η_s is the solvent viscosity and the density (ρ) terms refer to a polymer mass concentration. These changes (which were actually made so that the equation can be developed) enable the shift factor to be defined in terms of the portion of the solution viscosity that is contributed by the polymer. This reduced variables superpositioning relationship was first developed for dynamic measurements and has been shown to characterize the temperature shift-

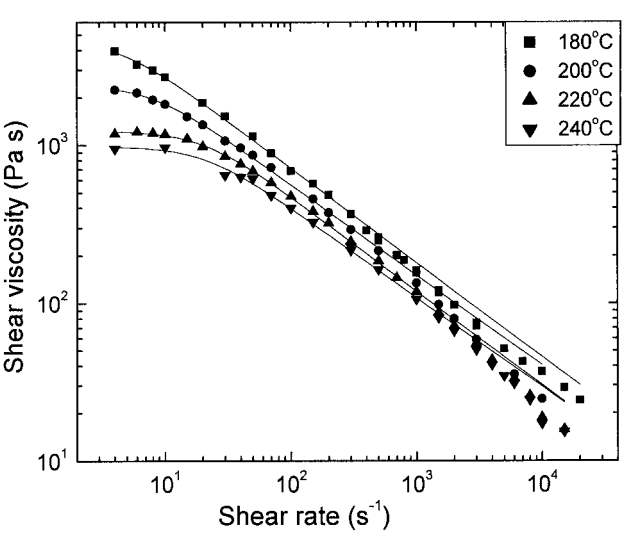

Figure 2 Shear viscosity data for HGX PP.

TABLE I
Carreau Model Parameters and Temperature Shift Factors (a_T)

Sample	Temperature	Carreau model parameters			a_T
		η_0 (Pa s)	λ (s)	n	
LDPE-E	175	12,867	9.78	0.62	2.41
	200	5,645	3.28	0.61	1
	225	3,039	2.28	0.65	0.511
	250	1,559	0.98	0.64	0.25
HDPE-B	175	50,267	13.98	0.5367	1.533
	200	36,775	10.32	0.5346	1
	225	19,452	4.47	0.5166	0.707
	250	19,488	4.07	0.4729	0.443
HGX PP	180	4,664	0.2327	0.4036	2.02
	200	2,410	0.129	0.430	1
	220	1,232	0.05	0.403	0.49
	240	982	0.048	0.433	0.3757

ing of the shear viscosity, complex viscosity, normal stress coefficients, and storage and elastic moduli and viscosities. It is further generally assumed for polymer melts that the ρ at T is equal to the ρ_0 at T_0 so that

$$a_T = \frac{\eta_0(T)T_0}{\eta_0(T_0)T} \tag{9}$$

The Carreau rheological model is given in eq. (10):

$$\frac{\eta - \eta_\infty}{\eta_0 - \eta_\infty} = [1 + (\lambda\dot{\gamma})^2]^{(n-1)/2} \tag{10}$$

where η_∞ is the infinite shear rate viscosity, λ is a time constant that is related to the λ_j in eq. (8), n is the power law exponent. Eq. (10) can be used to extrapolate the viscosity to a zero shear rate value (η_0). As a result, using the method of reduced variables, a master curve is formed by plotting a reduced shear viscosity (η_r) versus the reduced shear rate ($\dot{\gamma}_r$). Because the shear stress (τ_{ij}) is fairly insensitive to temperature, the shear strain rate is sensitive to temperature[8] and $\eta = \tau_{ij}/\dot{\gamma}_{ij}$, then the following definitions are typically made:[8]

$$\dot{\gamma}_r = a_T\dot{\gamma} \tag{11}$$

$$\eta_r = \eta(\dot{\gamma}, T)\,\frac{\eta_0(T_0)}{\eta_0(T)} \tag{12}$$

Rearranging eq. (9) and substituting into eq. (12) gives

$$\eta_r \doteq \frac{\eta(\dot{\gamma}, T)T_0}{a_T T} \tag{13}$$

The temperature dependence of a_T is often assumed to be an Arrhenius dependence as

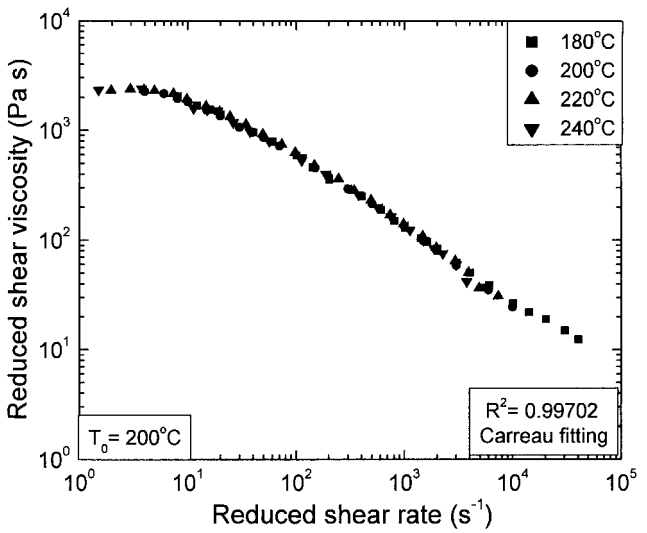

Figure 3 The master curve for the shear viscosity of HGX PP.

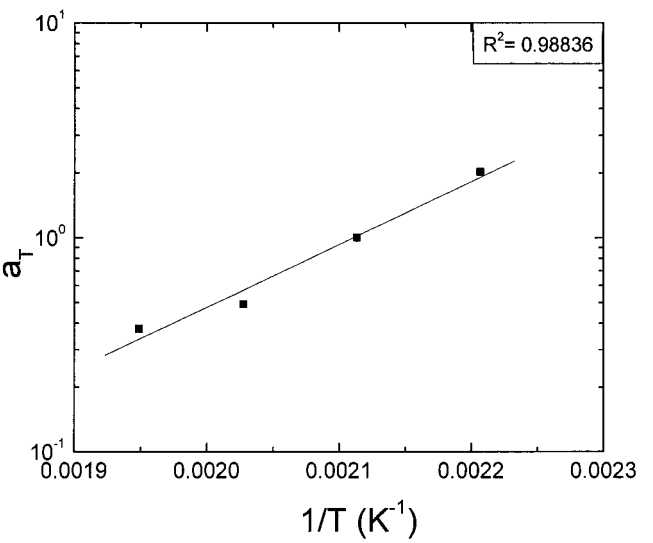

Figure 4 An Arrhenius plot for the shift factors of HGX PP.

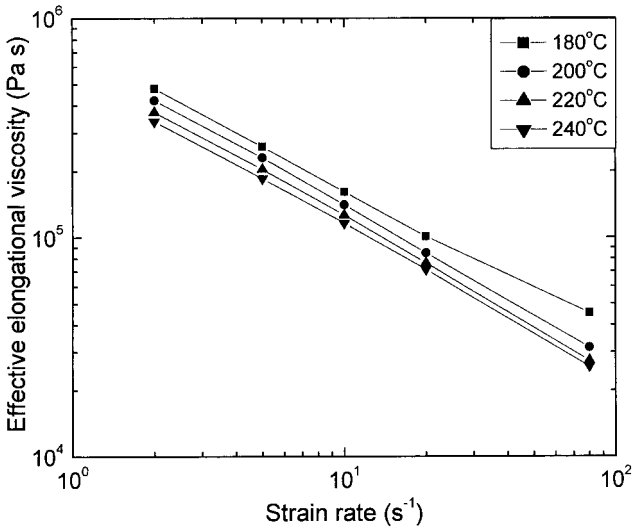

Figure 5 The effective elongational viscosity for HGX PP at Hencky 6.

$$a_T = \exp\left[\frac{\Delta H}{R}\left(\frac{1}{T} - \frac{1}{T_0}\right)\right] \quad (14)$$

where ΔH is the activation energy for flow and R is the universal constant.

The shear viscosity of an extrusion grade PP (HGX PP, Phillips HGX 030) versus the shear rate as a function of temperature is shown in Figure 2. The shift factors for this PP (given in Table I) are determined from the zero shear rate viscosities and by fitting the shear viscosity data with the Carreau model as shown in Figure 2. The data as shifted to a master curve is shown in Figure 3, and plots of ln a_T versus $1/T$ are given in Figure 4. The slope of the line in this figure indicates that $\Delta H/R$ is equal to 6731 K for HGX PP.

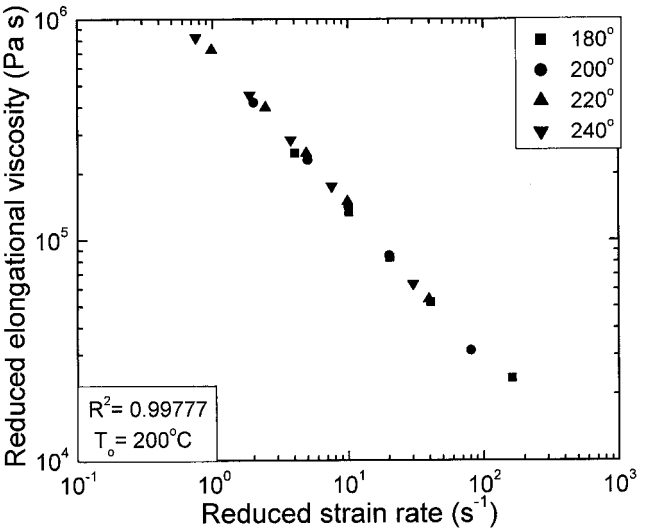

Figure 6 The reduced effective elongational viscosity for HGX PP at Hencky 6.

Temperature shifting for effective elongational rheology

It is assumed in this work that the elongational stress components (τ_{ii}) are insensitive to temperature, which was mentioned as common for the shear stress components. It is further assumed that the same shift factors determined from the extrapolated zero shear rate viscosities should also be the shift factors for elongational viscosities. Therefore, the $\dot{\gamma}$ values in eqs. (11), (12), and (13) would be replaced by the $\dot{\varepsilon}$, and the viscosity terms in these equations would be the η_{eff}. Figure 5 represents the data for this same HGX PP for η_{eff} versus $\dot{\varepsilon}$ at different temperatures and Hencky strain 6. As indicated by the master curve formed by shifting the effective elongational viscosity curves to T_0 = 200°C in Figure 6, the shear shift factors are also appropriate for convergent effective elongational viscosity data shifting.

Additional experimental data for the HGX PP and a complete set of data for two PEs are now presented to demonstrate the applicability of the shifting method.

EXPERIMENTAL

Materials

Experimental data on 10 samples of PEs and one PP are presented. The PP is an extrusion grade HGX 030 (Phillips) with a molecular weight of 300,000 and a polydispersity index of 5. The characteristics of the PE samples are presented in Table II.

Instruments and techniques

The shear and effective elongational viscosities were measured by using an ACER 2000 (advanced capillary

TABLE II
LDPE and HDPE Characteristics

Sample	Density (g/mL)	MW[a] (g/mol)	MWD[a]
LDPE-A	0.9	97,550	2.22
LDPE-B	0.9	56,950	1.99
LDPE-C	0.895	83,350	2.24
LDPE-D	0.919	86,650	6.85
LDPE-E	0.923	80,350	5.15
HDPE-A	0.943	105,200	9.74
HDPE-B	0.95	125,400	8.09
HDPE-C	0.954	125,700	13
HDPE-D	0.949	183,200	14.77
HDPE-E	0.949	154,100	12.63

MW, molecular weight; MWD, molecular weight distribution.

[a] Analyzed by GPC.

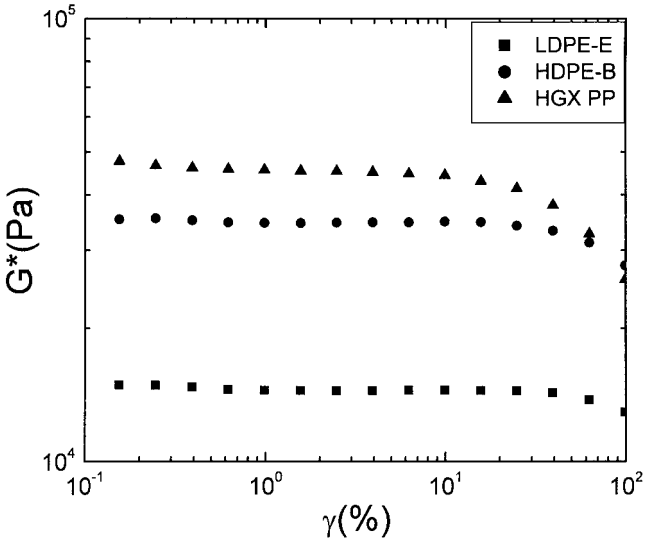

Figure 7 Dynamic strain sweep tests for LDPE-E, HDPE-B, and HGX PP.

extrusion rheometer, Rheometric Scientific) instrument. A capillary die with a 1-mm diameter and a length/diameter ratio of 20 was used for the shear viscosity and semihyperbolic dies of Hencky strains 4, 5, 6, and 7 were used for the measurement of the effective elongational viscosity. The chosen strain rates were calculated with eq. (15):

$$\dot{\varepsilon} = \frac{v_0}{L}(e^{\varepsilon_H} - 1) \tag{15}$$

where ε_H is the Hencky strain defined by eq. (7), v_0 is the velocity of the melt at the entrance cross-sectional area, and L is the length of the die. The steady-state melt pressure at the entrance of the die was used to calculate the effective elongational viscosity with eq. (6).

The complex viscosity was measured with an ARES (advanced rheometric expansion system, Rheometric Scientific) instrument by using parallel plate geometry (25-mm diameter and 1-mm gap). The linear viscoelastic region was previously tested by performing a dynamic steady-state strain sweep test. The complex modulus results as a function of strain for the HGX PP and two PEs are presented in Figure 7, which shows a linear region on most of the strain scale.

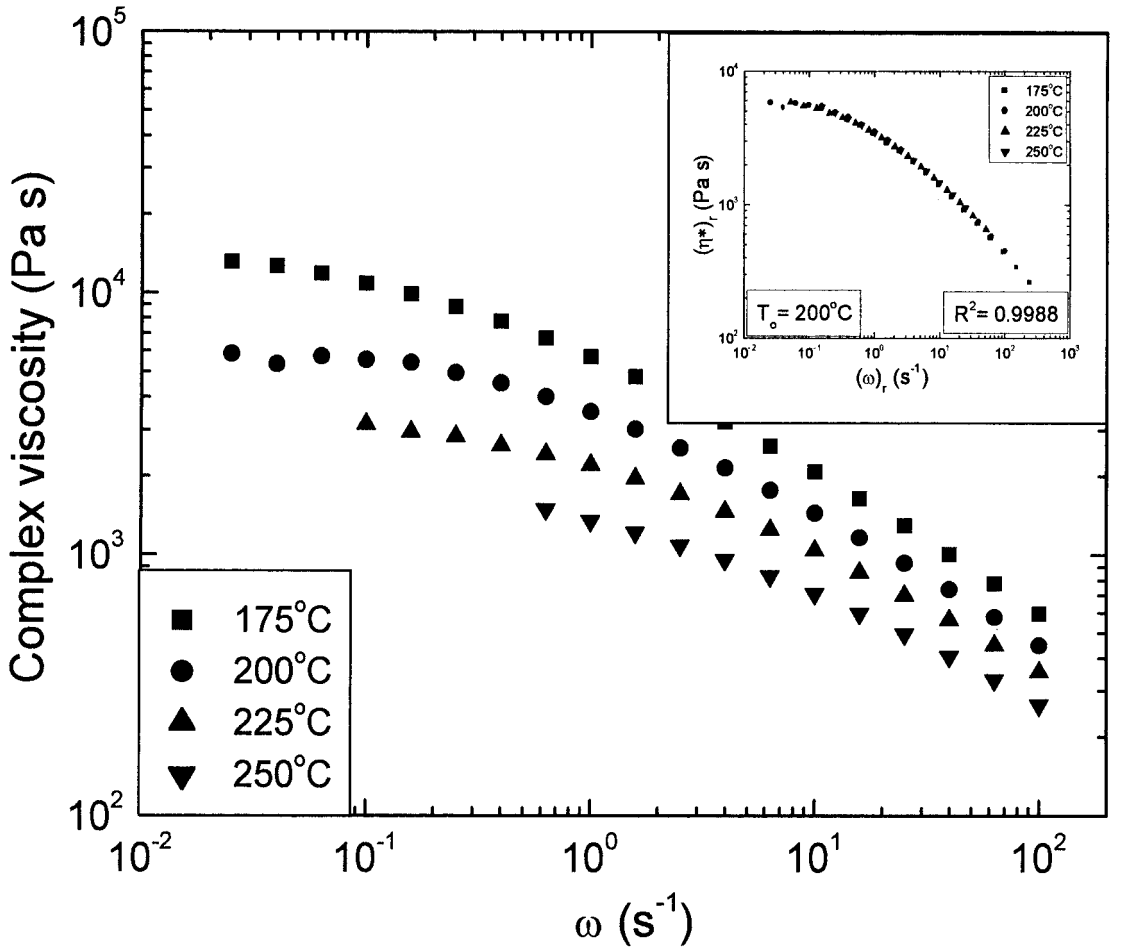

Figure 8 The complex viscosity and complex viscosity master curve for LDPE-E.

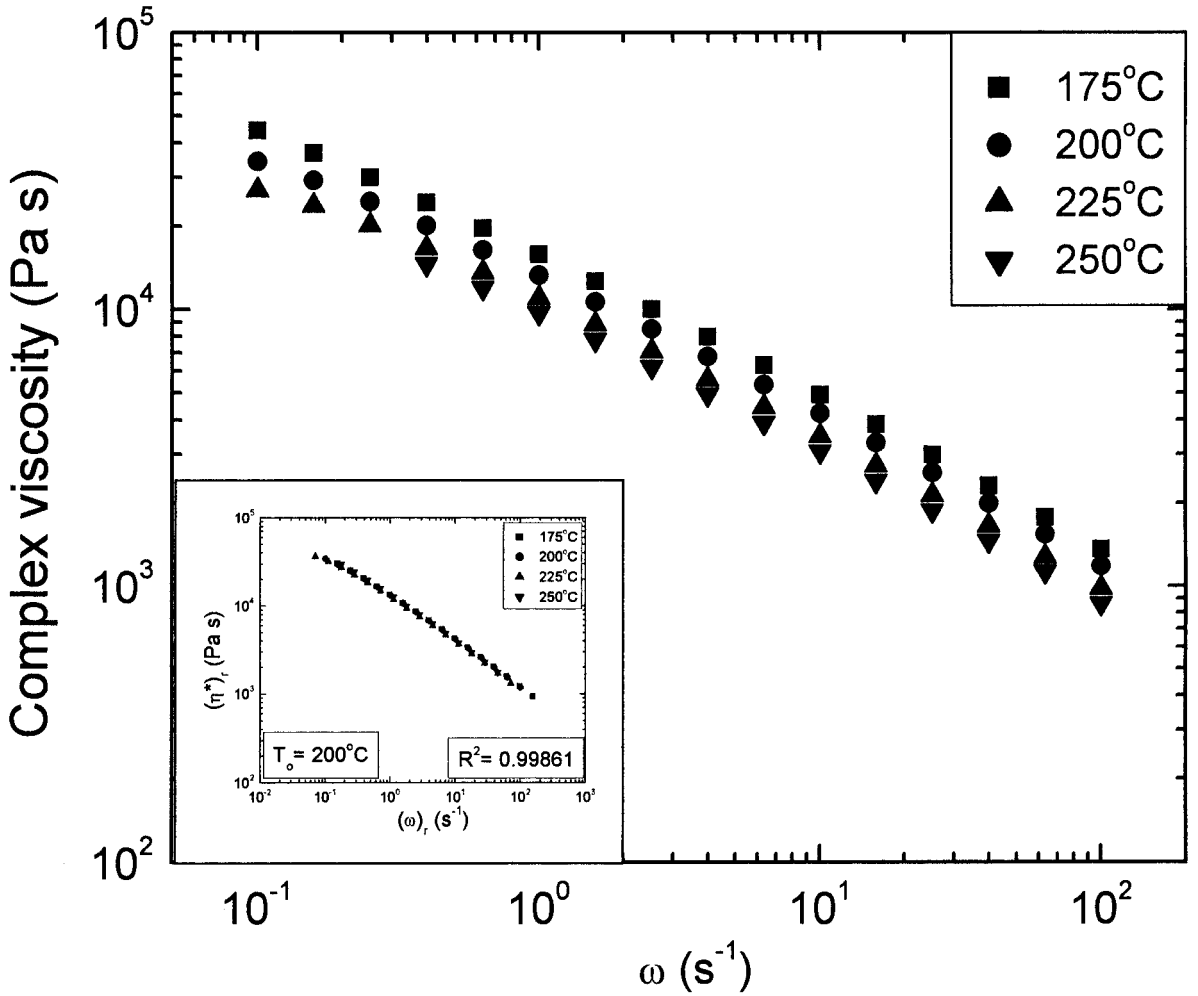

Figure 9 The complex viscosity and complex viscosity master curve for HDPE-B.

Similar results were obtained for the other samples of PEs. Dynamic sweep frequency tests at 1% strain were performed in order to measure the complex viscosity for all PE samples. Both shear (steady-state and/or dynamic) and elongational viscosity curves were obtained at four temperatures.

RESULTS AND DISCUSSION

The complex viscosity curves for the low density PE sample E (LDPE-E) and high density PE sample B (HDPE-B) are presented in Figures 8 and 9. By using the Carreau model, eq. (10), the parameters presented in Table I were fit, and then the temperature shift factors were calculated with eq. (9).

Shifting of the effective elongational viscosity curves was done by using the shift factors presented in Table I. The results for LDPE-E are given in Figures 10–14. The general trend of "strain rate thinning" is noticed for all tested temperatures. Increasing the Hencky strain brings about an increase of the effective elongational viscosity, irrespective of the strain rate or temperature. This is attributable to the higher body forces needed to induce the orientation of the macromolecular chains from the polymer melt sample at higher degrees of cross-sectional flow area reduction. The master curve for the elongational viscosity at Hencky 6 is shown in Figure 12, using the viscosity curve at 200°C as a reference curve. The same procedure was used to construct master curves for Hencky 4, 5, and 7 and the resulting master curves are presented in Figure 14. The shifting technique shows very good agreement, the coefficient of determination varying between 0.9963 and 0.99797.

The elongational viscosity for HDPE-B sample is presented in Figures 15–19, showing the same general trend of "elongation strain rate thinning" and "strain hardening" for all Hencky strains and temperatures. Increasing the Hencky strain determines a change of behavior with respect to temperature, as seen from Figures 17 and 18 at higher strain rate. The effect of temperature change is only noticed at intermediate

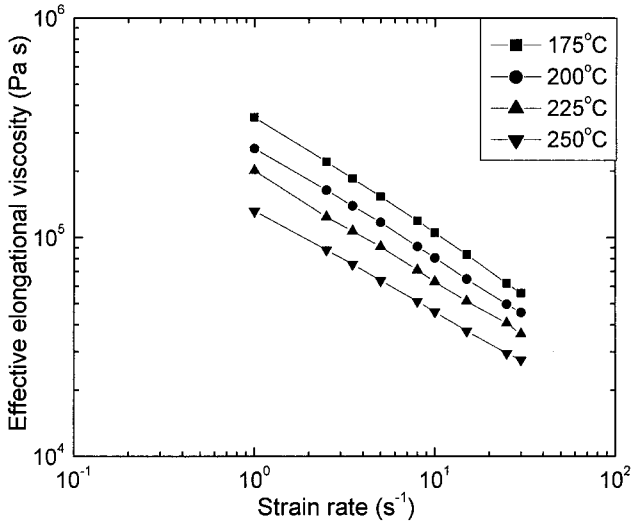

Figure 10 The effective elongational viscosity for LDPE-E at Hencky 4.

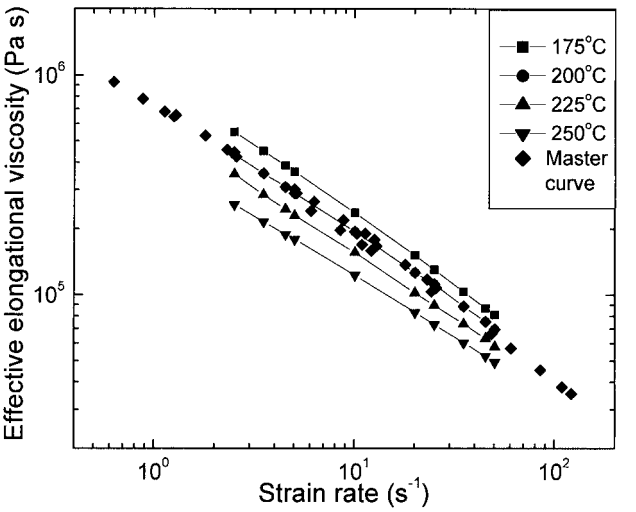

Figure 12 The effective elongational viscosity for LDPE-E at Hencky 6.

and lower strain rates. This behavior was also noticed for other HDPE samples.

The effective elongational viscosity master curves with respect to temperature for this sample of HDPE are shown in Figure 19. As compared to the LDPE-E sample, the effective elongational viscosity of the HDPE-B sample is higher, but the general trend is similar, the master curves for Hencky strains 4, 5, 6, and 7 being almost parallel with each other.

Figures 5 and 20–23 present the effective elongational viscosity curves for the HGX PP sample, which displays many interesting features. The first characteristic of this polymer sample is that the elongational viscosity shows a difference of the temperature effect as compared with the PE samples, particularly at high temperatures and Hencky strains, as seen from the almost compact and parallel pattern of the curves at temperatures between 200 and 240°C and Hencky strains 5, 6, and 7. At Hencky 4 the temperature sensitivity is higher and a trend toward a Newtonian region is noticed from the slopes of the curves in the range of lower strain rates. The effective elongational viscosity curves at 180°C and higher Hencky strains show a different pattern (i.e., a reduction of the slope as the strain rate is higher). Similar behavior is noticed in the case of shear viscosity at the same temperature and higher shear rates (see Fig. 2). The onset of the change in the general strain rate thinning behavior is noticed at a lower strain rate, as the Hencky strain is higher. This is probably due to the change in the

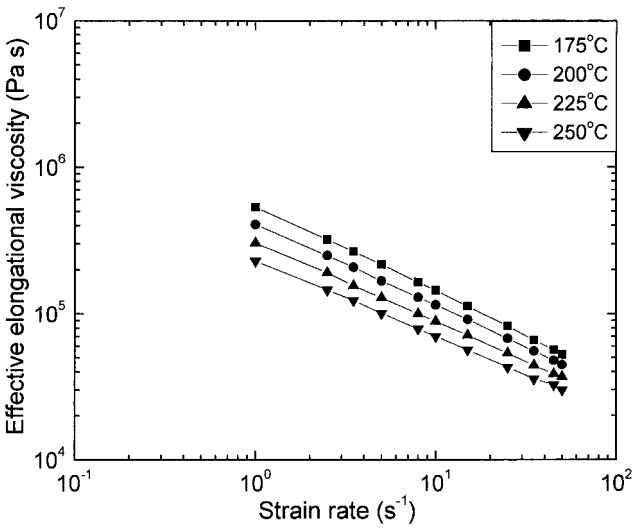

Figure 11 The effective elongational viscosity for LDPE-E at Hencky 5.

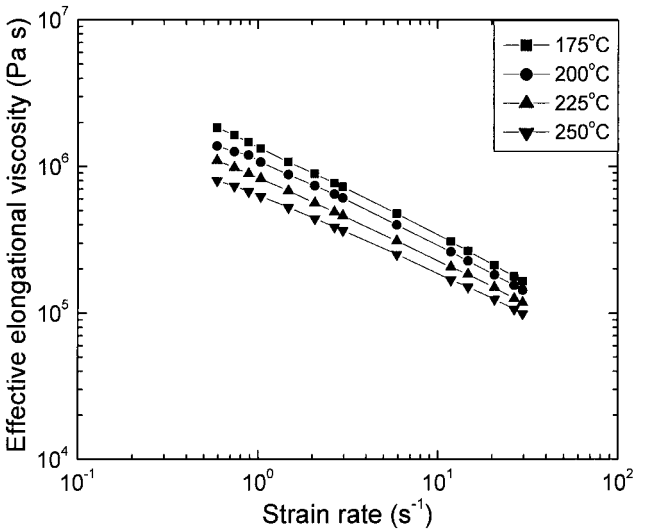

Figure 13 The effective elongational viscosity for LDPE-E at Hencky 7.

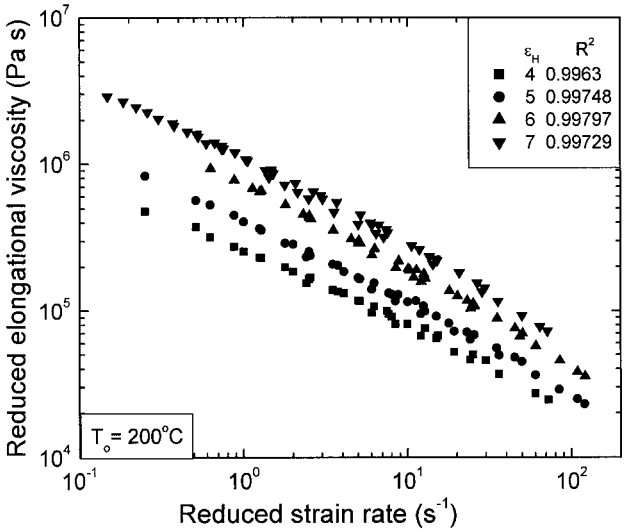

Figure 14 Master curves for the effective elongational viscosity of LDPE-E.

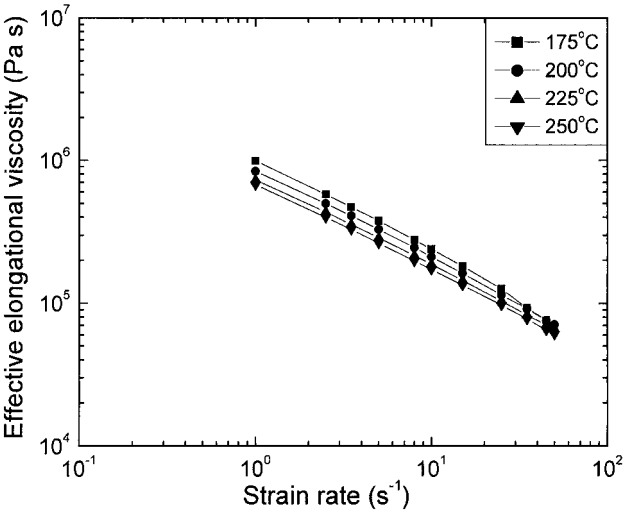

Figure 16 The effective elongational viscosity for HDPE-B at Hencky 5.

viscoelastic character of the melt at 180°C, a temperature close to the melting range for PP (155–172°C) according to DSC measurements. Shifting of the effective elongational viscosity curves for the HGX PP sample is shown in Figure 23; it shows the same parallel pattern of the master curves except at Hencky strain 4 and low strain rates and Hencky 6 and 7 at high strain rates.

The activation energies for elongational flow, as calculated with eq. (14), are given in Table III for all analyzed samples. The correlation between the activation energy and density and the molecular weight or molecular weight distribution is generally very poor, except the correlation between the activation energy and molecular weight ($R = -0.94519$) for HDPE and between the activation energy and density ($R = 0.96115$) for LDPE. Also, the data from Table III show that metallocene PE (samples LDPE-A to LDPE-C) has generally lower activation energies, as compared with Ziegler–Natta catalyzed PE (samples LDPE-D and LDPE-E). This may be explained by the difference in the polydispersity index for the two types of PEs. The lower sensitivity of the elongational viscosity to the variation of temperature in the metallocene catalyzed PE is due to the narrower molecular weight distribution. The same hypothesis seems to be valid in the Ziegler–Natta catalyzed PE.

A comparison of our data on the activation energy with that from the literature on activation energy for shear flow shows good agreement;[10–18] activation en-

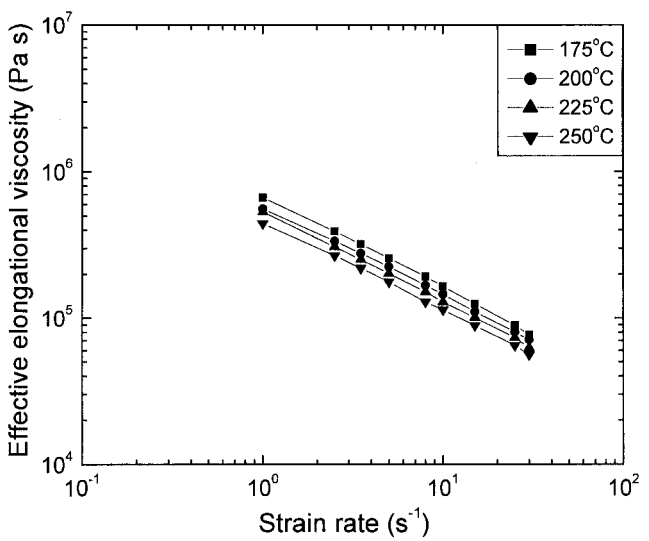

Figure 15 The effective elongational viscosity for HDPE-B at Hencky 4.

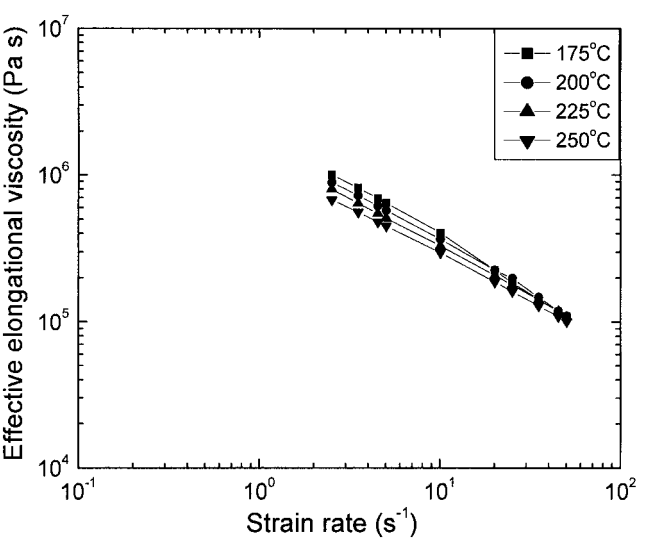

Figure 17 The effective elongational viscosity for HDPE-B at Hencky 6.

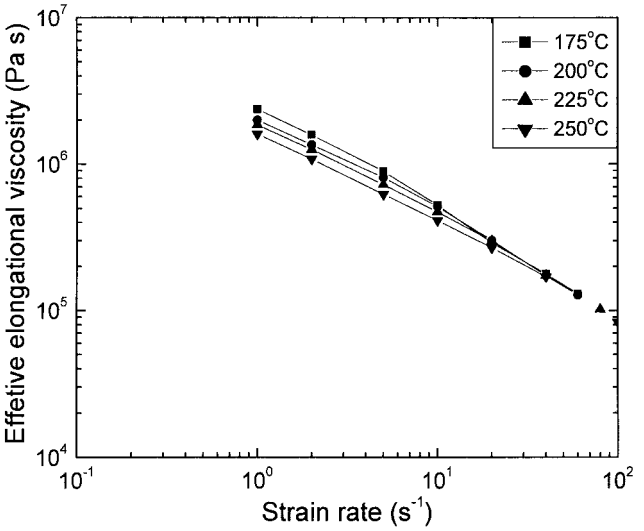

Figure 18 The effective elongational viscosity for HDPE-B at Hencky 7.

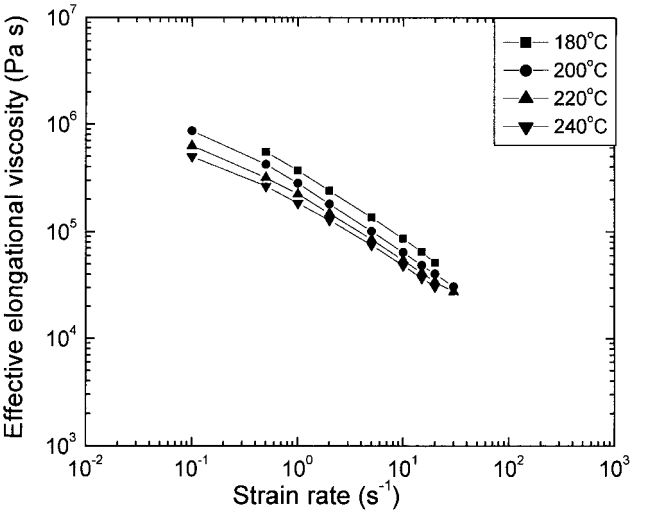

Figure 20 The effective elongational viscosity for HGX PP at Hencky 4.

ergies between 4.5 and 17 kcal/mol for PE and 8.5 and 21 kcal/mol for PP are reported. As our data show, the activation energy is higher for LDPE compared to HDPE[8,10,14,16–18] and higher for PP compared to PE.[8,11,15] Long chain branching increases the activation energy of PE.[19] To our knowledge, there are few reports in the literature on temperature shifting of the elongational viscosity curves to build a master curve. However, Münstedt and Middleman[20] reported that the temperature dependence of the elongational viscosity is the same as that of the shear viscosity with an activation energy of 13.088 kcal/mol for a LDPE. Wagner et al.[21] also reported activation energies for elongational flow of 10.048 and 5.622 kcal/mol for LDPE and HDPE, respectively.

CONCLUSIONS

Shifting of the effective elongational viscosity curves with respect to temperature was performed and master curves were constructed for different PEs and a PP. The effective elongational viscosity was measured by using the technique of convergent flow throughout semihyperbolic dies of different Hencky strains. The shear viscosity was also measured and shift factors were determined from the Carreau fitting based zero shear viscosities. The same shift factors were used to shift the effective elongational viscosity curves at different temperatures and build master curves for Hencky strains 4, 5, 6, and 7. The activation energy for shear and elongational flow was determined assuming Arrhenius dependence with the temperature. The

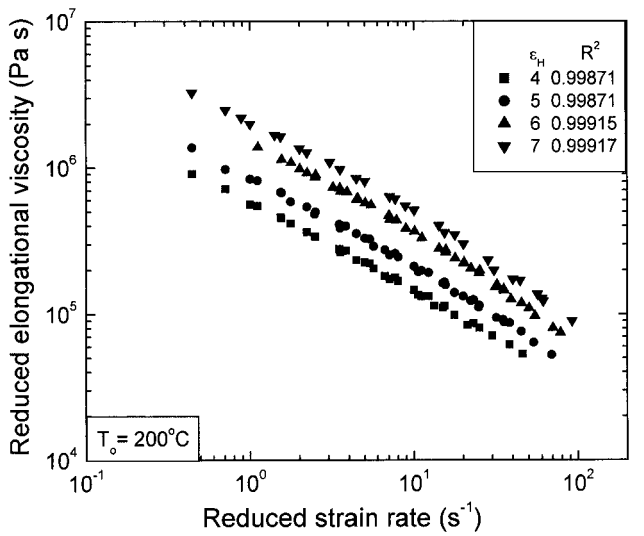

Figure 19 Master curves for the effective elongational viscosity of HDPE-B.

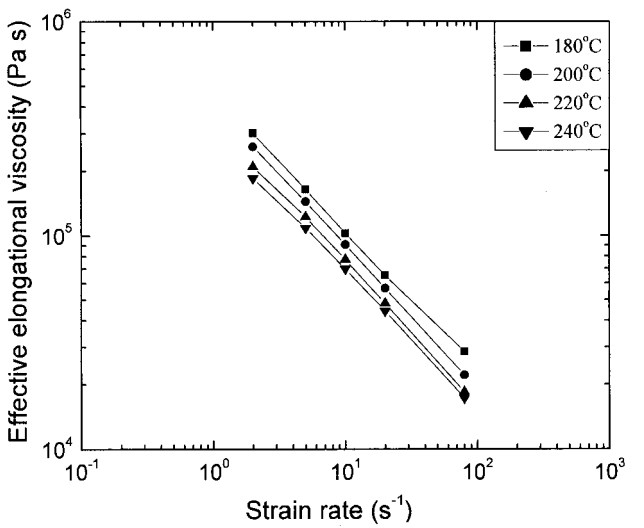

Figure 21 The effective elongational viscosity for HGX PP at Hencky 5.

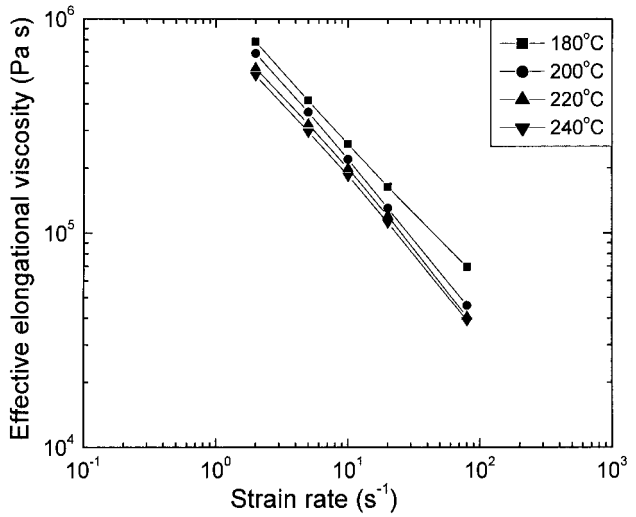

Figure 22 The effective elongational viscosity for HGX PP at Hencky 7.

range of activation energies for LDPE (6.098–13.88 kcal/mol), HDPE (4.631–7.541 kcal/mol), and PP (13.327 kcal/mol) are in good agreement with the literature data. In general, the activation energy is higher for LDPE compared to HDPE and is also higher for PP, if compared to that for PE. Metallocene catalyzed PEs show a lower activation energy that correlates with the lower polydispersity of these resins.

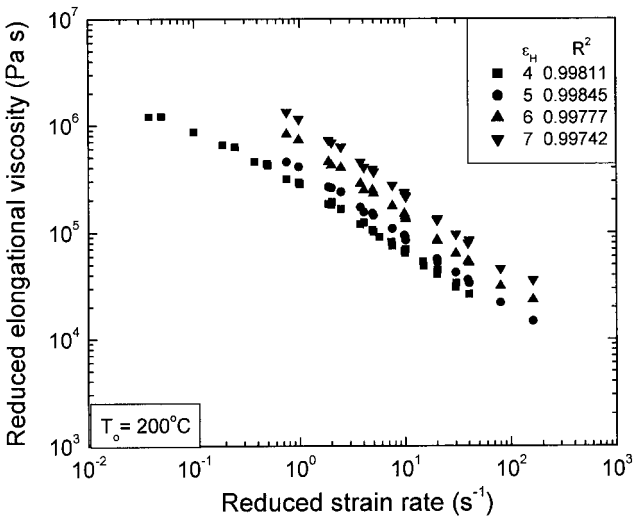

Figure 23 Master curves for the effective elongational viscosity of HGX PP.

TABLE III
Activation Energies for Elongational Flow

Sample	Density (g/cm^3)	MW[a] (g/mol)	MWD[a]	Activation energy (cal/mol)
LDPE-A	0.9	97,550	2.22	7,847
LDPE-B	0.9	56,950	1.99	7,284
LDPE-C	0.895	83,350	2.24	6,098
LDPE-D	0.919	86,650	6.85	10,605
LDPE-E	0.923	80,350	5.15	13,880
HDPE-A	0.943	105,200	9.74	7,410
HDPE-B	0.95	125,400	8.09	7,541
HDPE-C	0.954	125,700	13	6,975
HDPE-D	0.949	183,200	14.77	4,631
HDPE-E	0.949	154,100	12.63	4,851
HGX PP		300,000	5	13,327

MW, molecular weight; MWD, molecular weight distribution.
[a] Analyzed by GPC.

References

1. Collier, J. R.; Romanoschi, O.; Petrovan, S. J Appl Polym Sci 1998, 69, 2357.
2. Petrovan, S.; Collier, J. R.; Morton, J. H. J Appl Polym Sci 2000, 77, 1369.
3. Petrovan, S.; Collier, J. R.; Negulescu, I. I. J Appl Polym Sci 2001, 79, 396.
4. Seyfzadeh, B.; Collier, J. R. J Appl Polym Sci 2001, 79, 2170.
5. Collier, J. R. U.S. Pat. 6,220,083, 2001.
6. Collier, J. R. U.S. Pat. 5,357,784, 1994.
7. Ferry, J. D. J Am Chem Soc 1950, 72, 3746.
8. Bird, R. B.; Armstrong, R. C.; Hassanger, O. Dynamic of Polymeric Liquids. Fluid Mechanics, 2nd ed.; Wiley: New York, 1987; Vol. 1.
9. Bird, R. B.; Curtiss, C. F.; Armstrong, R. C.; Hassager, O. Dynamic of Polymeric Liquids. Kinetic Theory, 2nd ed.; Wiley: New York, 1987; Vol. 2.
10. Mendelson, R. A. Trans Soc Rheol 1965, 9, 53.
11. Wang, J.; Porter, R. S. Rheol Acta 1995, 34, 496.
12. Vinogradov, G. V.; Prozorovskaya, N. V. Rheol Acta 1964, 3, 156.
13. Gabriel, C.; Kaschta, J.; Münstedt, H. Rheol Acta 1998, 37, 7.
14. Tung, L. H. J Appl Polym Sci 1960, 46, 409.
15. Privalko, V. P.; Lipatov, Y. S. J Appl Polym Sci 1976, 14, 1725.
16. Miltz, J.; Ram, A. Polym Eng Sci 1973, 13, 273.
17. Chung, C. I.; Clark, J. C.; Westerman, L. In: Advances in Polymer Science and Engineering, Proceedings Symposia; Pae, K. D., Ed.; Plenum: New York, 1972.
18. Curto, D.; La Mantia, F. P.; Acierno, D. Rheol Acta 1983, 22, 197.
19. Huang, J.-C.; Liu, H.; Liu, Y. Polym Plast Technol Eng 2001, 40, 79.
20. Münstedt, H.; Middleman, S. J Rheol 1981, 25, 29.
21. Wagner, M. H.; Collignon, B.; Verbeke, J. Rheol Acta 1996, 35, 117.